5. Contract Specifications Book--Track Fastening Procurement. Contract X0-04-8. Mass Transit Administration, Baltimore, Md., Nov. 16, 1978.
6. Contract Specifications for Direct Fixation Fastener Procurement. Contract Y541--Stage I Rapid Transit System. Metropolitan Dade County Transportation Improvement Program, Miami, Fla., Jan. 1981.
7. O'Hare Extension Trackwork--Detail Specifications. Contract OE-21. Chicago Transit Authority, Chicago, Ill., March 1980.
8. Direct Fixation Fasteners Project Manual. Contract 2Z0085. Niagara Frontier Transportation Authority, Buffalo, N.Y., 1981.
9. Advanced Light Rapid Transit System. Metro Canada Limited, Vancouver, British Columbia, 1982.
10. Direct Fixation Rail Fasteners Procurement. Contract CQ833. Port Authority of Allegheny County, Pittsburgh, Pa., Aug. 1982.
11. Detroit Central Automated Transit System. Contract 3Z0663. Urban Transportation Development Corporation, Inc., Detroit, Mich., 1984.
12. Specifications for MBTA Contract No. 097-403 Systemwide Trackwork--Southwest Corridor Project. Massachusetts Bay Transportation Authority, Boston, 1983.
13. P. Witkiewicz. A Survey of Direct Fixation Fasteners Systems in North America--Existing Types and Associated Problems. Proc., Direct Fixation Fastener Workshop. Report UMTA-MA-06-0153-83-3. U.S. Department of Transportation, June 1985.
14. A. Sluz. Measurement of Direct Fixation Fastener Load Environment on the Washington Metropolitan Area Transit Authority Metrorail System. Proc., Direct Fixation Fastener Workshop. Report UMTA-MA-06-0153-83-3. U.S. Department of Transportation, June 1985.
15. Trackwork 10--Direct Fixation Fastener Procurement. Washington Metropolitan Area Transit Authority, Washington, D.C., July 1984.

Publication of this paper sponsored by Task Force on Rail Transit System Design.

The Reduction of Wheel/Rail Curving Forces on U.S. Transit Properties

CHARLES O. PHILLIPS and HERBERT WEINSTOCK

ABSTRACT

Summarized in this paper are recent government-sponsored studies to determine the effectiveness of various methods for reducing wheel/rail curving forces and resulting wear and component failure on U.S. transit properties. It describes the factors affecting the trade-off between curving performance and truck stability as it affects ride quality and the potential for derailment. A simplified description of truck-curving mechanics is presented, outlining three sources of lateral wheel/rail forces and three key methods for reducing those forces. References to more detailed papers and reports are included. Finally, the results of wheel/rail force measurements made for various truck and track configurations are presented and compared with theory. It is concluded that reductions in curving forces of up to 75 percent can be obtained by using tapered wheels and softening the longitudinal primary suspension or incorporating steerable trucks, or both.

Wheel/rail wear and related component failures have plagued transit systems since their inception at the turn of the century. In recent years, however, reports of such problems have occurred with increasing frequency. The Transportation Systems Center (TSC) sponsored by UMTA, U.S. Department of Transportation, has conducted studies and experiments to determine the causes and methods of reducing the incidence of high wear and component failure rates. Measuring wheel/rail wear and determining the factors that cause it are difficult and time-consuming. An interim step is to measure the wheel/rail forces that are a significant cause of the wear. Methods of reducing these forces can more rapidly be determined. Subsequently, the actual reduction in wear and component failures resulting from selected force reduction methods can be established over a longer period of

Transportation Systems Center, U.S. Department of Transportation, Cambridge, Mass. 02142.

time. Summarized in this paper is the result of the TSC's studies and experiments related to reducing wheel/rail forces. The paper (a) describes the stability versus curving performance of existing transit trucks; (b) provides an outline of curving mechanics; and (c) estimates the reduction in curving forces achieved by the use of tapered wheels, softening the longitudinal primary suspension, and incorporating steerable trucks.

BACKGROUND

New transit trucks introduced in the 1960s and 1970s to attract ridership with smooth, high-speed, comfortable performance proved to have high wheel/rail wear rates. Initially, transit engineers suspected high yaw resistance between truck and car body as a cause of wear because the new trucks supported the vehicle body through side bearers rather than through the center pins of the older design. Truck designers hastened to show that these forces were not high enough to account for the increase in wear. Through studies reported here, the main cause was determined to be the stiff elastomeric primary suspension elements incorporated to replace steel-spring, pedestal-type suspensions of the older designs. The use of elastomers enabled the longitudinal stiffness to exceed what was needed for dynamic stability at transit speed maximums of 60-70 mph. By softening the longitudinal suspension, curving forces could be reduced without reducing the stability to the point that it would affect ride quality or the potential for derailment. These theories have been subsequently verified by measurements and the revenue use of softened suspensions for periods exceeding 2 years at both the Port Authority Transit Corporation (PATCO) and the Washington Metropolitan Area Transportation Authority (WMATA).

Two other controversies existed. The first concerned cylindrical versus tapered wheels. Although railroads used only 1:20 tapered wheels, several transit systems had, in the past, resorted to cylindrical transit wheels. Work reported here shows that tapered wheels and, in particular, a worn Heumann tapered-wheel profile cause lower level wheel/rail forces and provide adequate stability for present truck designs.

The second controversy concerned the importance of providing sufficient superelevation in curves to allow balance speed for normal operations. Work reported here shows superelevation to be reasonably insensitive toward reducing curving forces and wear in the face of high frictional forces. Furthermore, it was pointed out that high superelevations at low speeds as encountered in reversing loops could cause derailment in the presence of minor track misalignment.

Finally, the Budd Company/H. List steerable truck designs, which were developed in part with UMTA program funding and which are presently in revenue service on the Philadelphia PATCO system, are compared under the same conditions and instrumentation with a conventional and softened suspension Budd Pioneer 3 truck.

TRUCK STABILITY VERSUS CURVING PERFORMANCE

The factors affecting the trade-off between truck stability and curving performance are the interaxle shear stiffness and the interaxle bending stiffness. The shear stiffness, as shown in Figure 1, is related to the resistance to lateral displacement between the two axles and is primarily affected by the primary suspension lateral stiffness. The bending

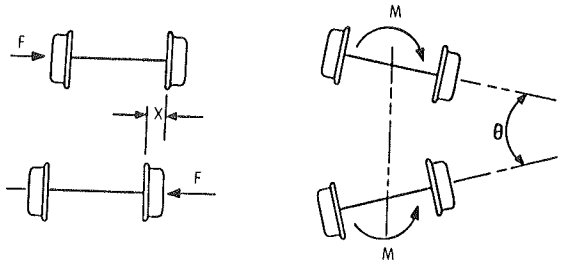

FIGURE 1 Schematic representation of generalized stiffness coefficients.

stiffness is related to the resistance to angular displacement between the two axles and is primarily affected by the primary suspension longitudinal stiffness.

Table 1 gives the stiffness of various transit trucks in current use on U.S. transit properties. Data on vertical stiffness affecting ground and truck vibration are included but not discussed here. Figure 2 shows some of these stiffnesses and relates them

TABLE 1 Transit Truck Suspension Stiffness Characteristics

Property	Manufacturer Truck	Vertical Stiffness (lb/in.)	Bending Stiffness (in./lb)	Shear Stiffness (lb/in.)
CTA	Wegmann	14,560	1.3×10^7	6.3×10^3
MARTA	Rockwell	150,000	1.2×10^8	2.6×10^4
MBTA-Blue	GSI	6,500	6.1×10^7	9×10^3
MBTA-Orange	GSI	7,500	7.3×10^7	10.7×10^3
PATCO	Budd	160,000	2.3×10^8	5.9×10^4
PATH	GSI	32,000	2.4×10^8	4.3×10^4
WMATA	Rockwell	90,000	1.3×10^8	1.8×10^4
WMATA	Breda	10,500	1.1×10^8	1.5×10^4

Note: CTA = Chicago Transit Authrotiy, MARTA = Metropolitan Atlanta Rapid Transit Authority, MBTA = Massachusetts Bay Transit Authority, PATCO = Port Authority Transit Corporation, PATH = Port Authority Trans-Hudson, and WMATA = Washington Metropolitan Area Transportation Authority,

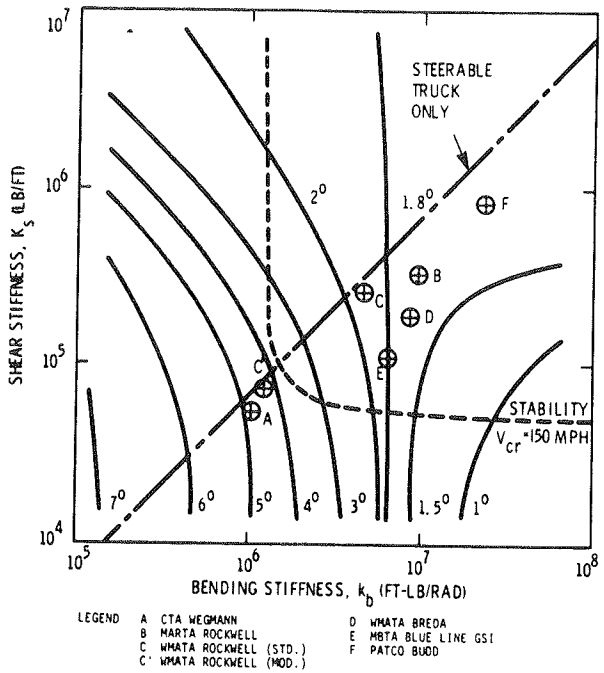

FIGURE 2 Truck curving and stability versus bending and shear stiffness (preliminary).

to truck curving performance and stability. Curving performance is indicated by the angular curvature in degrees that the truck can negotiate without hard flanging, which produces high wheel/rail wear. Stability is indicated by a single critical speed of 150 mph above which hunting and instability occur. As a comparison, the Chicago Transit Authority (CTA) Wegmann truck with a relatively soft suspension can negotiate a 5-degree curve without hard flanging and remain stable at speeds of less than 150 mph, but well above the CTA operating speed of 55 mph. The PATCO Budd truck with a stiffer suspension can negotiate a curve of only less than 1.8 degree without hard flanging and has a critical speed well above 150 mph, as compared with a maximum operating speed at PATCO of 75 mph.

This information is intended to be qualitative to allow comparison and to determine trade-off potential. It does not include the effects of varying the wheel profile, the wheel/rail adhesion coefficients, and the hard flanging. A more practical wear index based on the work performed is described later. Conventional trucks discussed fall below the diagonal line. Steerable trucks with interaxle connecting linkages allow greater freedom for performance trade-offs and can occur above as well as below the line.

Curving performance versus stability is discussed in greater depth in the literature (1).

TRUCK CURVING MECHANICS

Wheel-flange wear and rail gage-face wear result the lateral wheel/rail forces produced as a truck negotiates a curve. The causes of these forces have been imperfectly understood, resulting in a continuing controversy over the methods to reduce them. The following discussion is an attempt to outline in simple terms the present understanding of this phenomenon. It is broken down into seven conditions as follows:

- Condition A: Centrifugal Force
- Condition B. Pivot Force
- Condition C: Wheel/Rail Friction Force
- Condition D: Combined Forces
- Condition E: Tapered Wheels
- Condition F: Soft Suspension and Tapered Wheels
- Condition G: Steerable Truck

Three sources of lateral wheel/rail forces are described in Conditions A, B, and C. Condition D combines them for comparison and to represent the actual forces encountered during curving. Conditions E, F, and G describe three methods for reducing these forces.

Condition A: Centrifugal Force

Figure 3 shows the most easily understood component of curving (or centrifugal) force. To isolate this condition, the wheel/rail friction coefficient and the truck/carbody pivot torque are assumed to be zero. Under these conditions, the centrifugal force F_c acting outward on the car body is reacted by the lateral wheel/rail force F_l, acting inward on the four high-rail wheel flanges. The formula for F_c is presented as a function of the velocity v and the track superelevation E.

Figure 4 shows the wheel/rail force F_l acting on one truck at balance speed, where it is defined to be zero, and for an unbalance of 3 in., where it is calculated to be approximately 1,000 lb for an 80,000-lb car. For conditions where the friction coefficient is not assumed to be zero, the low-rail wheels as well as the high-rail wheels will take up the reactive force. It is assumed that the force would be divided equally among the eight wheels of the two trucks and that the resulting wheel/rail force, F_l, would then be reduced to 500 lb.

Condition B: Pivot Force

Figure 5 shows the second component of curving force, the truck/car body frictional pivot force. As a truck enters a curve and is forced to pivot in relation to the car body, the resulting resistance to turning is

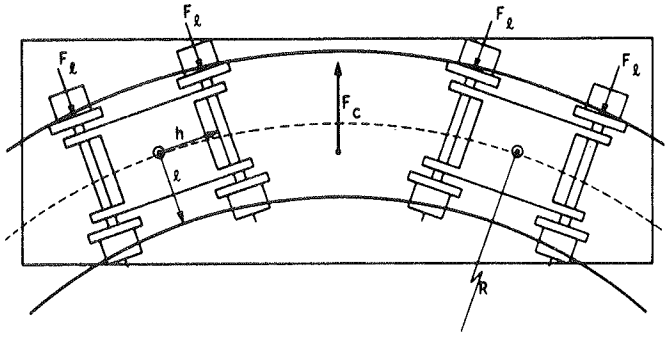

CENTRIFUGAL FORCE ON CAR

$Fc = W[\ v^2/gR - E/2\ell]$

LATERAL WHEEL/RAIL FORCE

$F\ell = Fc/4$

FRICTION COEFFICIENT $\mu = 0$ CONICITY $\alpha = 0$
TRUCK PIVOT TORQUE $T = 0$ SUSPENSION STIFF

W = CAR WEIGHT
V = VELOCITY
g = ACCELERATION OF GRAVITY
R = CURVE RADIUS
E = SUPER ELEVATION
ℓ = 1/2 TRACK GAGE
h = 1/2 TRUCK WHEEL BASE

FIGURE 3 Condition A: centrifugal force.

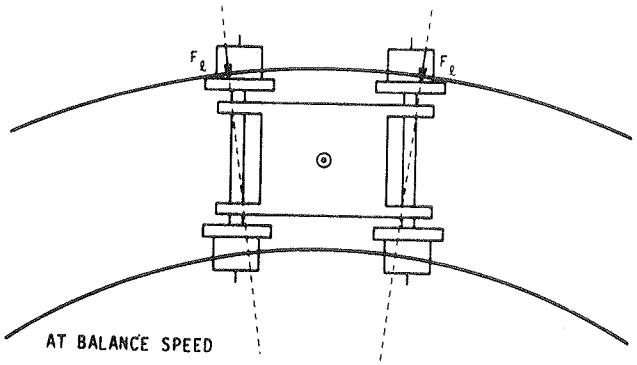

AT BALANCE SPEED

$F\ell = 0$

WITH AN UNBALANCE OF 3" FOR $\mu = 0$

$F\ell = 0.05\ W/4 = 0.05 \times 80{,}000$ LBS./4 = **1,000 LBS.**

FOR $\mu = \mu^*$

$F\ell = 0.05\ W/8 = 0.05 \times 80{,}000$ LBS./8 = **500 LBS.**

FRICTION COEFFICIENT $\mu = 0$ CONICITY $\alpha = 0$
TRUCK PIVOT TORQUE $T = 0$ SUSPENSION STIFF

FIGURE 4 Condition A: centrifugal force (wheel/rail force F_1 acting on one truck at balance speed).

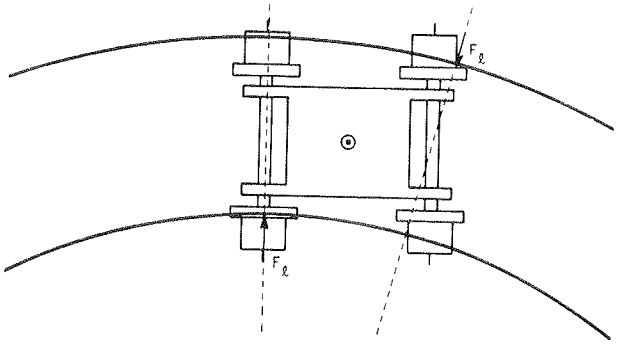

LATERAL WHEEL FORCE AT BALANCE SPEED

$F\ell = T/2h$

$F\ell$ = 80,000 INCH-LBS./2 x 43 INCHES = **1,000 LBS.**

TRUCK PIVOT TORQUE $T = T^*$ CONICITY $\alpha = 0$
FRICTION COEFFICIENT $\mu = 0$ SUSPENSION STIFF

FIGURE 5 Condition B: pivot force.

reacted by the lead-axle, high-rail wheel and the trailing-axle, low-rail wheel for the lead truck and by the opposite wheels for the trailing truck. To isolate and simplify this phenomenon, the friction coefficient is assumed to be zero. The truck pivot torque is assumed to be 80,000 in.-lb, and the half-gage width is assumed to be 43 in., based on measured data for the WMATA sidebearing Rockwell truck (2). Under these conditions, the lead truck high-rail lateral wheel force is calculated to be approximately 1,000 lb. In the constant radius portion of the curve, this force would be zero, except for fluctuations attributed to track geometry and wear irregularities. As the truck leaves the curve, the forces are reversed.

Condition C: Wheel/Rail Friction Force

Figure 6 presents the most important and most poorly understood component of curving force, the wheel/rail friction force. To isolate this condition, the truck is assumed to be operating at balance speed and the truck pivot torque is assumed to be zero. The friction coefficient is assumed to be 0.5. Under wet or lubricated conditions, the friction coefficient is lower. As a result of the wheel/rail friction force,

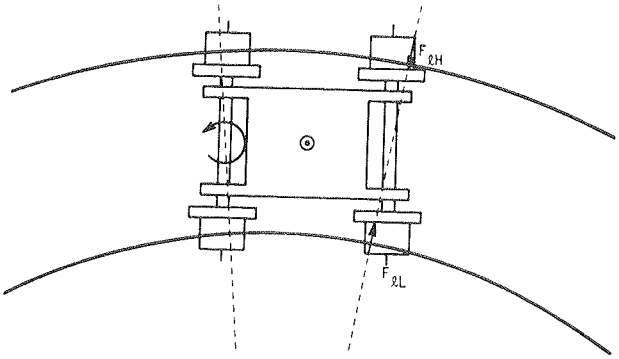

LATERAL WHEEL FORCE AT BALANCE SPEED

HIGH RAIL	LOW RAIL
$F\ell = 1.2\ \mu W/8$	$F\ell = \mu\ W/8$
$F\ell = 1.2 \times 0.5 \times 80{,}000$ LBS./8 =	$F\ell = 0.5 \times 80{,}000$ LBS./8 =
6,000 LBS.	**5,000 LBS.**

FRICTION COEFFICIENT $\mu = \mu^*$ CONICITY $\alpha = 0$
TRUCK PIVOT TORQUE $T = 0$ SUSPENSION STIFF

FIGURE 6 Condition C: wheel/rail friction force.

t.. d-axle, high-rail wheel experiences an inward force of approximately 6,000 lb and the low-rail wheel an outward force of 5,000 lb, as calculated for an 80,000-lb transit car with a friction coefficient of 0.5. These forces decrease with increasing radius but are reasonably independent of speed. They can be accounted for as follows.

The trailing axle assumes an almost radially aligned position, but in the absence of wheel taper, a moment is created because of the greater distance to be traveled by the outside high-rail wheel versus the inside low-rail wheel. This moment is transmitted by the truck frame to the lead axle, which causes the high-rail wheel to flange against the high rail and create a high angle of attack for both the high- and low-rail wheels. This angle of attack causes lateral forces to be created, acting outward on the treads of the low- and high-rail wheels as the wheels tend to go straight rather than curve. These combined forces are reacted by the inward flange force on the high-rail wheels as they contact the gage side of the high rail. The result of the outward tread force and the more-than-twice-as-great inward flange force is an inward high-rail wheel force as previously defined. These forces pushing inward on the wheels of the leading axle are reacted by spreading forces outward on the rails. This complex wheel/rail interaction is described in much greater detail in the literature (3).

Condition D: Combined Forces

Figure 7 shows the combination of the lateral wheel forces as previously described. Although in actual-

LATERAL WHEEL FORCES FOR A 3-INCH UNBALANCE FOR μ = 0.5

CONDITION	Fℓ HIGH RAIL	%	Fℓ LOW RAIL
A	500	7	-500
B	1,000	13	0
C	6,000	80	5,000
D	7,500 LBS.	100	4,500 LBS.

LATERAL WHEEL FORCES AT BALANCE FOR μ = 0.5

CONDITION	Fℓ HIGH RAIL	%	Fℓ LOW RAIL
A	0		0
B	1,000	14	0
C	6,000	86	5,000
D	7,000 LBS.	100	5,000 LBS.

FRICTION COEFFICIENT $\mu = \mu^*$ CONICITY α = 0
TRUCK PIVOT TORQUE T = T* SUSPENSION STIFF

FIGURE 7 Condition D: combined forces.

ity these forces are interactive and not directly additive, they are simply added here for comparative purposes.

The total lateral wheel rail force on the lead axle of the lead truck for a 3-in. unbalance is 7,500 lb for the high rail and 4,500 lb for the low rail. For balance conditions with centrifugal forces reduced to zero, the forces are 7,000 lb and 5,000 lb, respectively. The pivot force is assumed to be positive as it increases the flange force on the high-rail wheel and to not affect the nonflanging low-rail wheel.

As can readily be seen, the wheel/rail friction force of Condition C predominates. For small radius curves and high coefficient of friction, it can be 80-90 percent of the total force, with the result that lateral wheel/rail force during curving are insensitive to speed and not significantly affected by superelevation. This contradicts a theory accepted by a least some people and properties in the industry but is verified by the studies and experiments reported here. [For further discussion, see report by Grief and Weinstock (3).]

Condition E: Tapered Wheels

As shown in Figure 8, introducing tapered wheels reduces the lateral wheel/rail friction force on the high-rail wheel as much as 30 percent, as measured at the WMATA system in Washington, D.C. (6,7). The condition presented here assumes balance speed for a zero centrifugal force, as described in Condition D.

This force reduction is caused by the reduction in the moment on the trailing axle because the tapered wheel allows the high-rail wheel to travel further with less slippage than does the cylindrical wheel. A similar moment on the leading axle is also reduced, further reducing the high-rail, lead-axle lateral force.

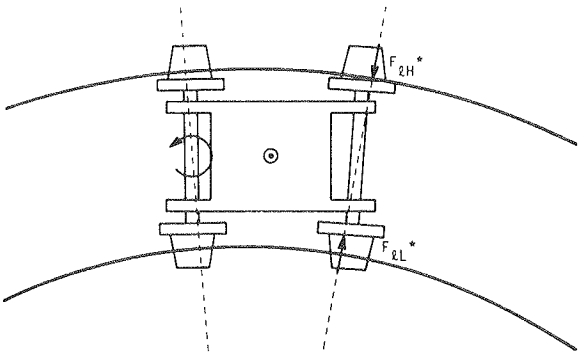

LATERAL WHEEL FORCE AT BALANCE

Fℓ = 0.30 x 6,000 LBS. + 1,000 LBS. = 2,800 LBS.

SUSPENSION SOFT FRICTION COEFFICIENT $\mu = \mu^*$
CONICITY $\alpha = \alpha^*$ TRUCK PIVOT TORQUE T = T*

FIGURE 9 Condition F: soft suspension and tapered wheels.

Condition F: Soft Suspension and Tapered Wheels

As shown in Figure 9, a softened longitudinal primary suspension in addition to tapered wheels reduces the lateral wheel/rail friction force on the high rail as much as 70 percent, as measured at the WMATA system in Washington, D.C. (6). The same assumptions of balance and pivot force are made as in Condition E.

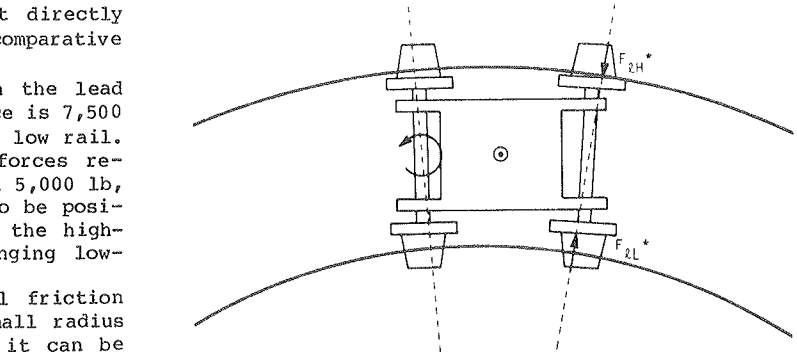

LATERAL WHEEL FORCE AT BALANCE

Fℓ = 0.70 x 6,000 LBS. + 1,000 LBS. = 5,200 LBS.

CONICITY $\alpha = \alpha^*$ FRICTION COEFFICIENT $\mu = \mu^*$
SUSPENSION STIFF TRUCK PIVOT TORQUE T = T*

FIGURE 8 Condition E: tapered wheels.

This significant reduction is caused by the tendency toward radial alignment of both the leading and trailing axles that is allowed by the reduction in longitudinal or bending stiffness, as previously described. On the trailing axle, this change in alignment occurs naturally because of the moment between the axle and the frame of the truck. The radial alignment of the lead axle is less obvious and is caused by (a) the combination of a couple between the lead and trailing axle and (b) the flange contact of the high-rail wheel beneath the running surface of the track, creating a forward force on the axle at the high-rail wheel.

Condition G: Steerable Truck

Figure 10 shows the steerable truck condition created by further softening of the longitudinal suspension and interconnecting the axles with steering arms or linkages to allow complete radial alignment of the axles. Under ideal conditions with sufficient taper and large radius curves, the wheel/rail friction forces can be reduced to practically zero. Allowance is still made here for the pivot force needed to align the axles while entering or leaving the curve. For small radius curves, the self-steering truck shown here is unable to generate sufficient force to align the axles. By interconnecting the linkages with the car body, a forced steering configuration

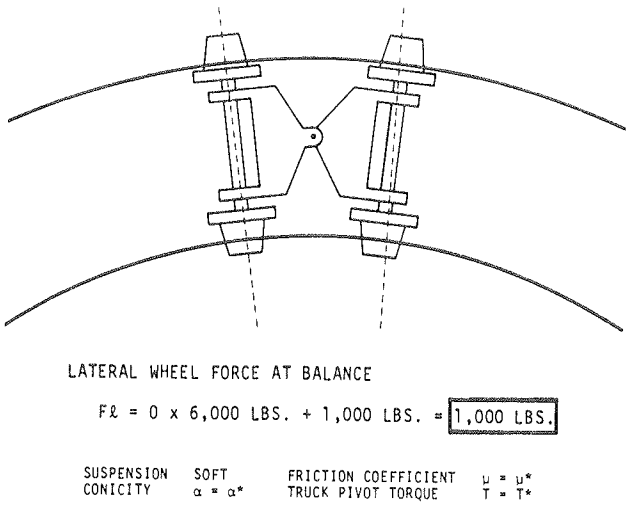

FIGURE 10 Condition G: steerable truck.

is created that provides additional force for radial alignment. Because practical tapers cannot allow for the negotiation of small-to-medium curves without wheel slippage, wheel/rail friction forces are still significant, even with forced steering.

MEASUREMENT AND MODELING RESULTS

Figure 11 shows lateral wheel/rail force as a function of speed as measured on the tight turn loop, a 150-ft radius test curve at the Transportation Test Center in Pueblo, Colorado. It demonstrates the insensitivity to speed predicted by the wheel/rail friction-force component described under Condition C. Forces of 9,000 lb on the high-rail wheel and 6,000 lb on the low-rail wheel are in reasonable agreement with the general condition described under Condition D. The computer predictions presented here are described in greater detail in the literature (7).

Figures 12 and 13 show lateral wheel/rail force as a function of track curvature in degrees as measured by WMATA. They demonstrate the significant reduction in forces accomplished by changing from a cylindrical-wheel, stiff primary-suspension truck configuration to a tapered-wheel, soft primary-suspension truck. The computer predictions are described in greater detail in the literature (8).

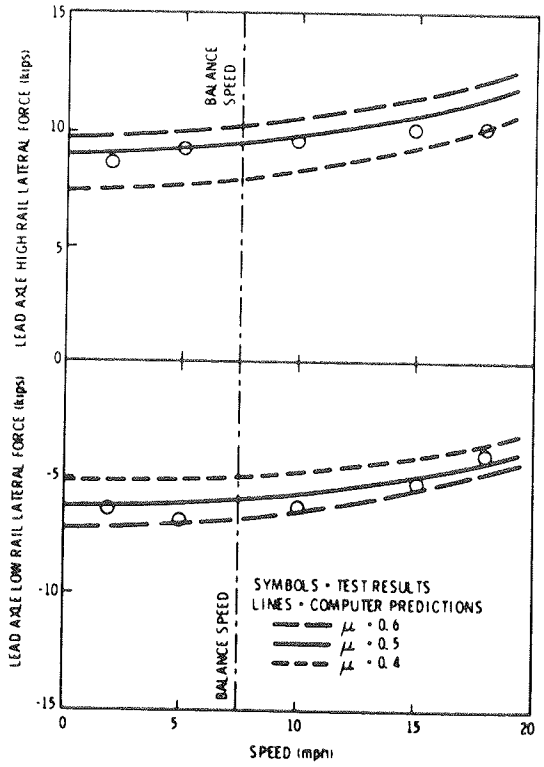

FIGURE 11 Lead axle, high and low rail, lateral force speed with a 150-ft curve radius.

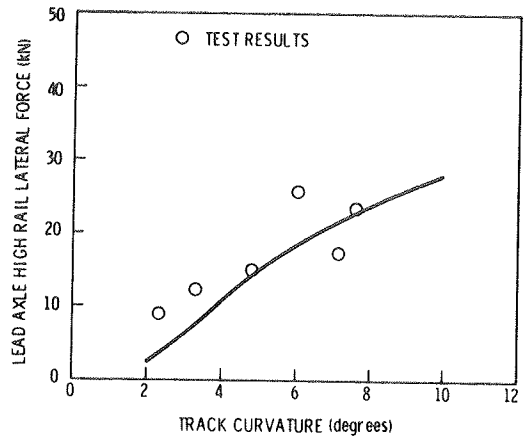

FIGURE 12 Comparison of lateral wheel/rail force predictions versus test results—cylindrical wheel, stiff suspension.

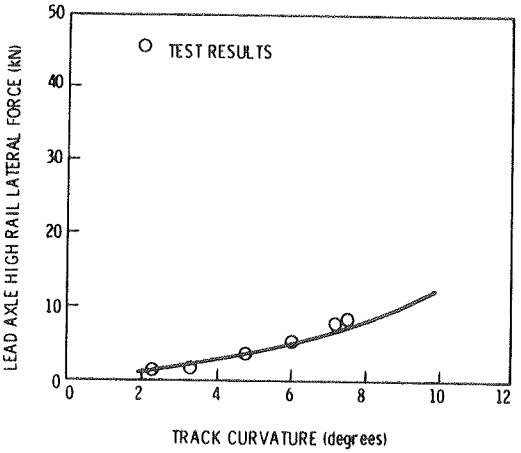

FIGURE 13 Comparison of lateral wheel/rail force predictions versus test results—tapered wheel, soft suspension.

Figure 14 shows a summary of the results from the WMATA wheel/rail force measurement made to compare tapered and cylindrical wheel profiles with the conventional stiff suspension and the experimental soft suspension. Maximum force reductions of 70 percent are observed. It is interesting to note the higher forces for curve 311 on a 1,000-ft radius curve. These forces are significantly higher for all but the tapered soft-suspension configuration because curve 311 is in the offside location from the other curves. Small-but-measurable axle misalignments ac-

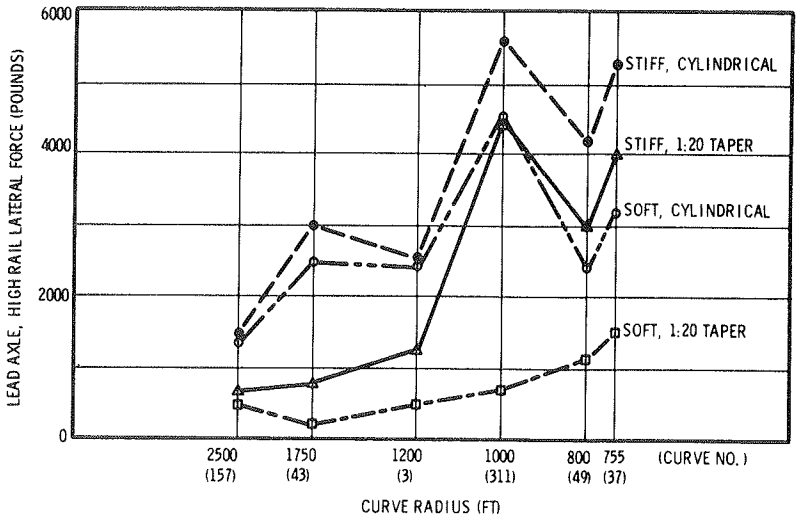

FIGURE 14 Summary of results from WMATA truck test project (for balance speed conditions).

count for a preference for the truck to curve in one direction versus the other (2,6).

Figure 15 shows a sample of actual, measured, high-rail, wheel/rail force data as a function of distance through curve 37, a 7-degree curve. The highly irregular non-steady-state force fluctuations observed are shown to correlate with the gage-face wear pattern presented above the force data. The power spectral density of each, plus their cross-spectral density, are presented at the lower left of the figure. The high correlation with a peak of approximately 41 ft is indicated. This peak is close to the welded-rail section length of 39 ft. The cause for these fluctuations has not been determined. Most likely, track geometry variations are a prime cause with truck/track dynamics emphasizing or deemphasizing the magnitude and frequency of the fluctuations.

Figure 16 shows predicted lateral wheel/rail force as a function of track curvature in degrees for a baseline conventional truck versus a self-steering truck and forced-steering truck. For the same condition, Figure 17 shows the work at the flanging wheel, which is calculated from the creep forces and the resultant creep vectors in the contact path between the wheel and the rail. This calculation of work is proposed as a wear index to relate wheel/rail force with predicted wear of wheels and rails. It is the leading outer wheel that is responsible for the

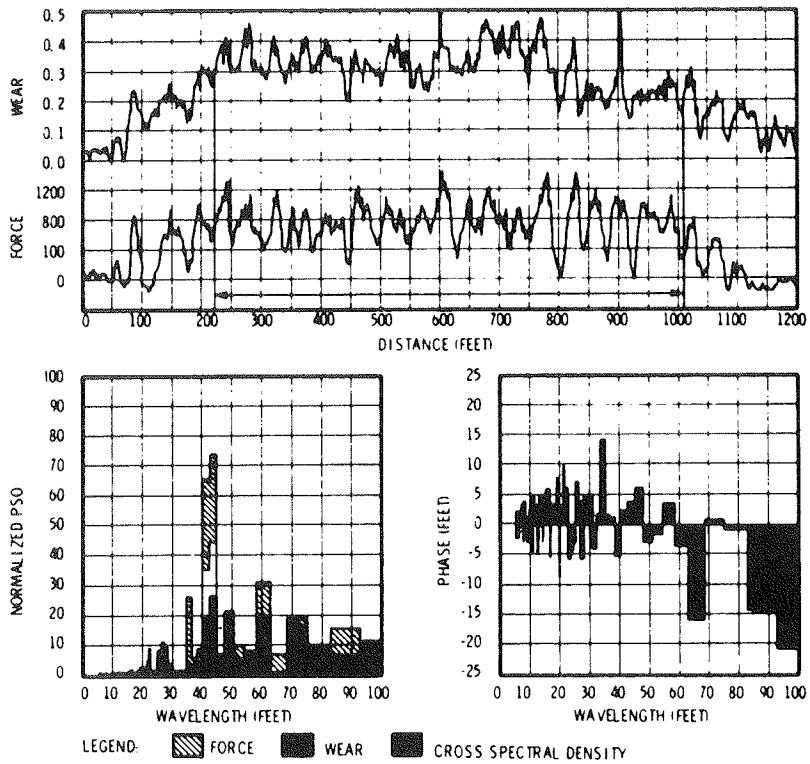

FIGURE 15 Comparison of lateral wheel/rail forces versus gage face wear—curve 37, high-rail, tapered-wheel, stiff suspension at 40 mph.

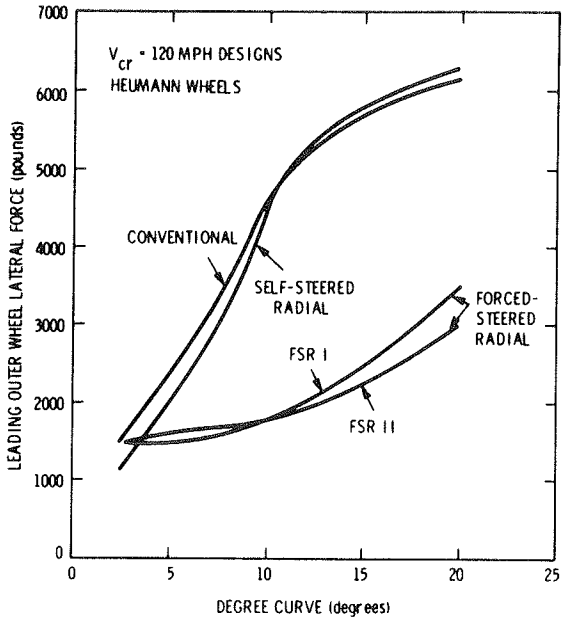

FIGURE 16 Leading outer wheel lateral force versus curvature for baseline truck designs with Heumann tapered wheels (critical speeds = 120 mph).

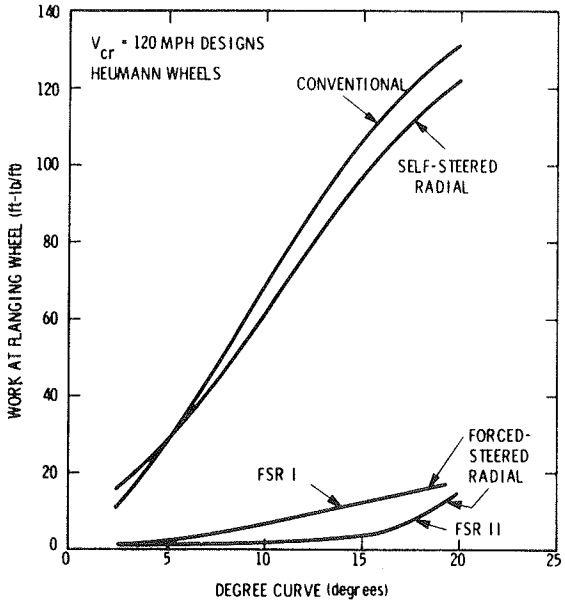

FIGURE 17 Work at flanging wheel versus curvature for baseline truck designs with Heumann tapered wheels (critical speeds = 120 mph).

vast majority of the wear that takes place on the gage face of the high rail and on the wheel flange. [Note that the predictions presented in Figures 16 and 17 are described in greater detail by Wormley et al. (1).]

Figure 18 shows data similar to Figure 15 for measurements made at the Philadelphia PATCO system (9) on a 7-degree, westbound curve comparing a conventional suspension, a soft-suspension retrofit (in revenue services), and a steerable truck (in revenue service). These measurements are given in Table 2.

The soft suspension produces a 69 percent average force reduction and the steerable truck configuration produces a 75 percent average force reduction. Measurements made on the eastbound track of the same curve did not produce significant force reductions for either the soft or the steerable configurations. This is attributed to an ascending grade eastbound versus a descending grade westbound. Application of power on the ascending grade may longitudinally compress the suspension or linkages, or both, thus preventing proper axle steering and the reduction of lateral wheel/rail forces. This phenomenon was not observed on the WMATA system tests.

A further observation of the data revealed that the steerable truck wheelset in the trailing position produced significant forces, leaving curves unlike either the conventional or soft-suspension truck configuration. Finally, it was observed that the steerable truck produced reasonably high forces when negotiating curves with restraining rail and lubrication. The kinematics and dynamics of four-point contact appear to reduce the effectiveness of the steering mechanism. Figure 19 shows a summary of the wheel/rail force measurements versus curvature of the WMATA standard and soft-suspension trucks and the PATCO standard, soft-suspension steerable truck configurations.

The Rockwell truck at WMATA had a measured primary longitudinal suspension stiffness of 460,000 lb/in. per truck for the standard configuration and 120,000 lb/in. per truck for the suspension configuration. For a 7-degree (750-ft radius) curve at WMATA, a 75 percent reduction in suspension stiffness resulted in a 65-70 percent force reduction. At PATCO, an 80 percent reduction in suspension stiffness resulted in a 50 percent force reduction on a curve of the same radius. The steerable truck produced a 70 to 75 percent force reduction under the same conditions. It is interesting to note that the slope of the steerable configuration plot is significantly less than the other plots, indicating reduced curving forces for higher degrees of curvature. The soft-suspension configuration shows reduced forces in mild curves. This may be due to its ability to adjust to the irregularities in track geometry and gage-face wear profiles in contrast to the standard and steerable truck configurations.

As a result of these measurement and analysis activities, WMATA and PATCO will each retrofit 10 car sets (80 suspensions) in the fall of 1985. Further retrofits are being prepared for Baltimore

TABLE 2 PATCO Force Measurement, Westbound 7-Degree Curve

Truck Configuration	Longitudinal Stiffness (lb-in./trucks x 10^3)	Average Force (lb x 1,000)	Maximum Force (in.)	Standard Deviation
Conventional stiff	1,180	5.3	11.6	1.6
Retrofit soft	144	1.9	7.1	1.0
Steerable	N/A	1.3	6.2	0.8

Note: NA = not applicable

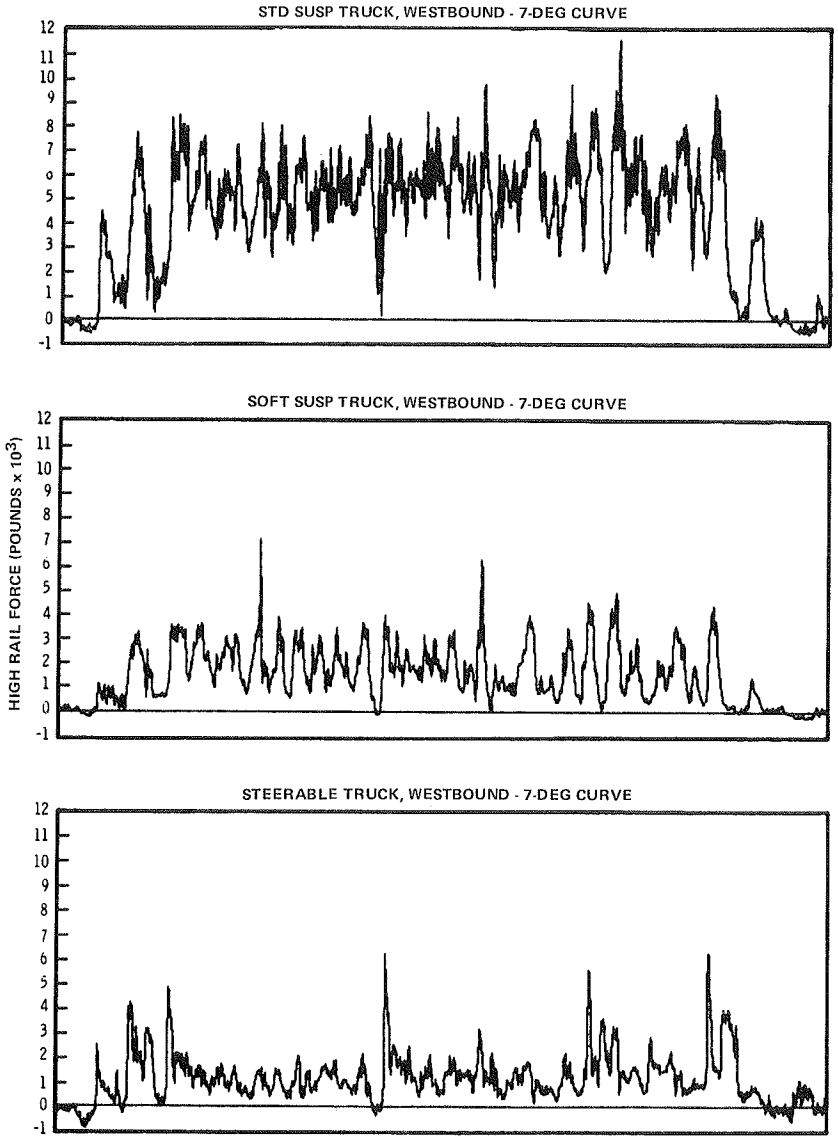

FIGURE 18 PATCO wheel/rail force measurement—standard, soft-suspension steerable configurations.

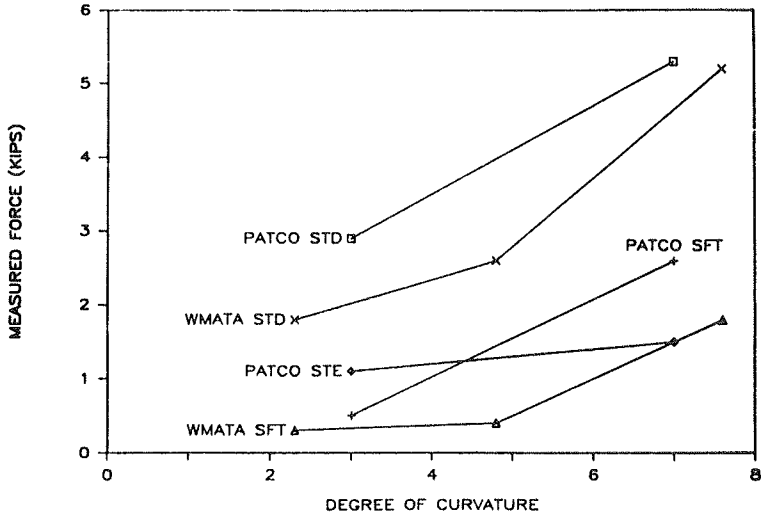

FIGURE 19 Wheel/rail force versus curvature—standard, soft-suspension steerable configurations.

and Amtrak. It is anticipated that successful fleet demonstrations will show a cost benefit if all vehicles with this type of suspension are retrofitted.

Although the steerable truck has been successfully demonstrated under revenue service at PATCO, its benefits at higher cost are not significantly better than the soft suspension configuration. No decision has been made to order more steerable trucks. It has been suggested that the true benefit of a steerable truck can best be realized on a new system specifically designed to make use of its advantages. The Vancouver/Urban Transportation Development Corporation steerable truck-equipped system should be closely monitored as an example of this condition.

REFERENCES

1. D.N. Wormley, J.K. Hedrick, and N.L. Nagurka. Stability and Curving Performance of Conventional and Advanced Rail Transit Vehicles. Report UMTA-MA-06-0025-83-10. UMTA, U.S. Department of Transportation, 1983.
2. J.A. Elkins. Wheel/Rail Force Measurements at the Washington Metropolitan Area Transit Authority--Phase II, Volume 1, Analysis Report. Report UMTA-MA-06-0025-83-1. UMTA, U.S. Department of Transportation, 1983.
3. R. Grief and H. Weinstock. Mechanics of Steady-State Curving: Relation Between Wheel-Rail Forces and Superelevation. Report 83-RT-6. ASME, New York, 1983.
4. C. Phillips, H. Weinstock, R. Grief, and W.I. Thompson. Measurement of Wheel/Rail Forces at the Washington Metropolitan Area Transit Authority--Volume 1, Analysis Report. Report UMTA-MA-06-0025-80-6. UMTA, U.S. Department of Transportation, 1980.
5. D.R. Ahlbeck, H.D. Harrison, and J.M. Trenten. Measurement of Wheel/Rail Forces at the Washington Metropolitan Area Transit Authority--Volume II, Test Report. Report UMTA-MA-06-0025-80-7. UMTA, U.S. Department of Transportation, 1980.
6. P.J. Boyd, J.P. Zaiko, and W.L. Jordon. Wheel/Rail Force Measurements at the Washington Metropolitan Area Transit Authority--Phase II, Volume II, Test Report. Report UMTA-MA-06-0025-83-2. UMTA, U.S. Department of Transportation, 1983.
7. J.A. Elkins, J. Peters, G.E. Arnold, and B.R. Raykumor. Steady State Curving and Wheel/Rail Wear Properties of a Transit Vehicle on the Tight Turn Loop. Report UMTA-CO-06-0009-83-1. UMTA, U.S. Department of Transportation, 1983.
8. J.A. Elkins and H. Weinstock. The Effect of Two Point Contact on the Curving Behavior of Railroad Vehicle. Report 82-WA/DSC-13. ASME, New York, 1982.
9. G. Mekosh. Measurement and Prediction of Wheel/Rail Forces at PATCO. Presented at 1985 Rapid Transit Conference, American Public Transit Association, Washington, D.C.

Publication of this paper sponsored by Task Force on Rail Transit System Design.